



# PROPERTIES AND STRUCTURE OF CIRCUMFERENTIAL JOINTS OF TUBES MADE BY ORBITAL ELECTRON BEAM WELDING

E.G. TERNOVOJ, V.F. SHULYM, A.R. BULATSEV, T.G. SOLOMIJCHUK and V.A. KOSTIN  
E.O. Paton Electric Welding Institute, NASU, Kiev, Ukraine

The paper presents investigations of the properties and structure of metal in circumferential joints of tubes from 304SS steel, PT-3V titanium alloy and monel alloy, produced by the method of orbital electron beam welding in vacuum. Performed investigations were focused on application of equipment and technology of orbital electron beam welding for repair of piping located outside functioning space objects.

**Keywords:** *piping, position butts, orbital electron beam welding, joints, 304SS steel, PT-3V titanium alloy, monel alloy, mechanical properties, macro- and microstructures, microhardness, chemical inhomogeneity*

Problem of welding position butts of various purpose piping is urgent for performance of repair operations on board the International Space Station (ISS) in space. Analysis of long-term operation of space facilities under the conditions of an orbital flight, in particular, of Russian orbital complex «Mir» reveals that one of the most vulnerable elements is technological piping which can fail during long-term operation for various reasons (mechanical damage, impact of meteorite particles, etc.) and can require repair under the conditions of space [1–4]. One part of the piping is inside the functioning modules, the other is located outside the station and is operating in the space vacuum at below zero temperatures. It is anticipated that after 6–10 years since the beginning of ISS operation a need may arise for their repair and for processes and devices for its implementation, accordingly.

Many years of research conducted at PWI demonstrated that the most acceptable method for repair of piping located inside the space modules, is TIG welding process in specialized put-on chambers with a controllable atmosphere [5–8], and for repairs outside the station this is electron beam welding [3, 4, 8].

TIG welding is usually used to weld butt joints with filler material feed or over flanges. Overlap joints, as well as circumferential joints of tubes made by multipass autoprodding method, are welded without filler material, their strength being not lower than that of joints welded with feeding of filler wire of matching composition [9–13].

In EBW of circumferential joints in one pass (without edge flanging) a depression forms on the weld face that essentially lowers the joint mechanical properties. In this connection, it is of interest to produce a sound butt joint of tubes by EBW process without feeding filler material and with reinforcement of the weld root and top part.

This paper gives the results of studying the properties and structure of tube joints made at retrofitting the technology of single- and two-pass orbital EBW without addition of filler materials, to produce vacuum-tight, strong and sound welded joints in order to solve the problems of pipeline repair in open space.

Experiments were performed using a laboratory power unit with electron beam heater that was rotating around a stationary tube (Figure 1). Samples were butt welded in a single pass or two passes, without addition of filler materials. Tubes of 12.8 mm diameter with 1.0 mm wall thickness from stainless steel 304SS, PT-3V titanium alloy and NMZhMts nickel alloy (monel) were used as samples. Optimum modes of orbital EBW, properties and structural features of the produced welded joints of tubes were determined.

Quality of the produced joints was assessed by external examination, checking the vacuum tightness of the joints with helium leak detector TI-1-14; rupture testing of tubes in TsDM-10 machine at the temperature of +20 °C, and in IMP machine at –196 °C temperature; flattening tests for ductility to GOST 8695–75 in TsDM-10 machine; investigations of macro- and microsections of the joints. Composition of base metal and weld metal was determined by spectral analysis using photoelectric spectrometer DFS-36.

Metallographic examination of the geometry and metal structure both of the entire joint and its individual sections was conducted in «Neophot-32» optical microscope. Joint microhardness  $HV1.0$  MPa was measured on longitudinal sections of tubes in the LECO microhardness meter M-400 with 200  $\mu\text{m}$  step. Structural components of 304SS steel were revealed by electrochemical etching in 20 % water solution of chromic acid at 10 V voltage for 5 s, and components of titanium alloy PT-3V were revealed by chemical etching in a reagent of the following composition: 1 volume fraction of HF; 3 volume fractions of  $\text{HNO}_3$ , 6 volume fractions of  $\text{H}_2\text{O}$ . Structure of monel alloy was revealed by electrochemical etching in 20 % water solution of ammonia sulphate at 20 V voltage for 5 s.



**Table 1.** Modes of orbital EBW for circumferential butt joints of tubes of  $\varnothing 12.8 \times 1.0$  mm

#	Material	$I_b$ , mA	$U$ , kV	$v_w$ , m/h	$t_1$ , s	$t_2$ , s	$t_3$ , s
1	304SS	35.0	9.2	22	0.5	14.0	3.0
2	PT-3V	32.5	9.5	36	1.5	8.0	3.5
3	Monel	35.0	9.2	15	1.0	16.0	3.0

Note.  $t_1$  – time for reaching working parameters;  $t_2$  – time of welding at working parameters;  $t_3$  – time of fading out.

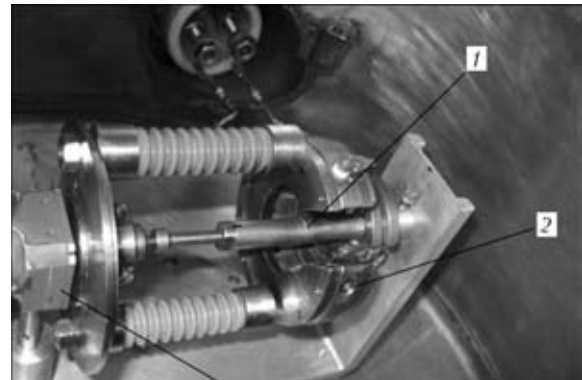


**Figure 1.** Test sample of electron beam heater for orbital EBW of butt joints of tubes: 1 – welded sample; 2 – circular electron beam heater; 3 – orbital revolution drive

Quantity of  $\delta$ -ferrite in the weld metal and base metal of welded joints was determined by ferritometer Ferrit Gehaltmesser-1.053. Chemical inhomogeneity of base metal and weld metal was studied in the Cameca microanalyzer SX-50.

Conducted experiments enabled determination of optimum modes of orbital EBW of circumferential joints of tubes from steel 304SS, titanium alloy PT-3V and monel alloy at up to 400 W beam power. Accelerating voltage, beam current, welding speed and time intervals of welding cycle were selected depending on tube material. Here accelerating voltage, beam current and welding speed are identical both for single- and two-pass welding. Welding mode parameters are given in Table 1.

Analysis of macrosections of tubes from 304SS steel, PT-3V alloy and monel alloy (Figure 2) showed that selection of welding modes enables achievement of optimum geometry and satisfactory formation of the upper and root reinforcement beads without addition of filler materials. Checking of welded joints for vacuum tightness did not reveal any violation of tightness of welds made with different number of passes.

It should be also noted that the composition of weld metal in joints of the above materials does not

differ from initial composition of base metal (Table 2), and is independent on the number of passes.

Obtained results of rupture testing of single-pass joints (Table 3) of tubes from steel 304SS at testing temperatures of  $+20$  °C were equal to  $(0.74-0.77)\sigma_t^{b.m.}$ , and for sample welded in two passes it was  $0.95\sigma_t^{b.m.}$ . At testing temperatures of  $-196$  °C these values increased by 10–15 % both for base metal and for welded joints compared to values obtained at  $+20$  °C temperature. Strength values of joints from monel alloy are similar to those of joints from 304SS steel. For titanium alloy PT-3V rupture testing was performed only at the temperature of  $+20$  °C. Having analyzed the results of the conducted testing, it should be noted that the highest strength values were found in two-pass joints that did not have any depressions of the weld upper bead.

During flattening tests of welded joints and base metal no cracks were found on samples from 304SS steel and monel alloy, whereas on samples from titanium alloy PT-3V longitudinal cracks were detected in base metal tubes and welded joints (Figure 3).



**Figure 2.** Macrosections ( $\times 20$ ) of butt welded joints produced by orbital EBW in two passes: a – steel 304SS; b – titanium alloy PT-3V; c – monel alloy

**Table 2.** Composition (wt.%) and values of tensile strength of the studied alloys

Material	C	Mn	Cr	Ni	Si	P	Cu	Fe	Al	V	Mo	Zr	Ti	$\sigma_t$ , MPa
304SS	0.2	2.0	18–20	8.0–10.5	1.0	0.045	–	Base	–	–	–	–	–	800
PT-3V	–	0.04	$\leq 0.1$	–	0.07	–	–	0.5	3.6	2.4	$\leq 0.3$	0.05	Base	810
Monel	–	1.2	–	Base	$< 0.2$	–	30.5	2.0	–	–	–	–	–	680



**Table 3.** Values of tensile strength of circumferential joints of tubes produced by orbital EBW

Studied section	Material	Number of passes	$\sigma_t$ , MPa, at $T$ , °C		Fracture site
			+20	-196	
Base metal	304SS	–	798	923	BM
Welded butt joint		1	620	812	WM
		2	760	915	HAZ
Base metal	PT-3V	–	800	–	BM
Welded butt joint		1	460	–	WM
		2	712	–	HAZ
Base metal	Monel	–	670	780	BM
Welded butt joint		1	560	680	WM
		2	630	740	FZ

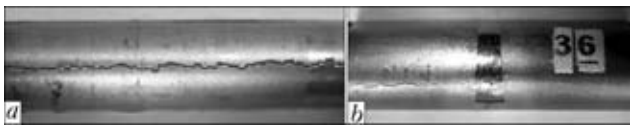


**Figure 3.** Samples of welded joint of titanium alloy PT-3V after flattening tests: *a* – base metal; *b* – orbital two-pass welding

Fracture of base metal samples of PT-3V alloy (in the form of cracks from both sides) occurred along the entire length of its generatrix. In welded samples cracks initiated also from both sides on the end faces and stopped on the boundary of base metal and HAZ. The weld and HAZ on both sides of the weld turned out to be so ductile that they acted as crack arresters (Figure 3, *b*). This is attributable to the fact that in

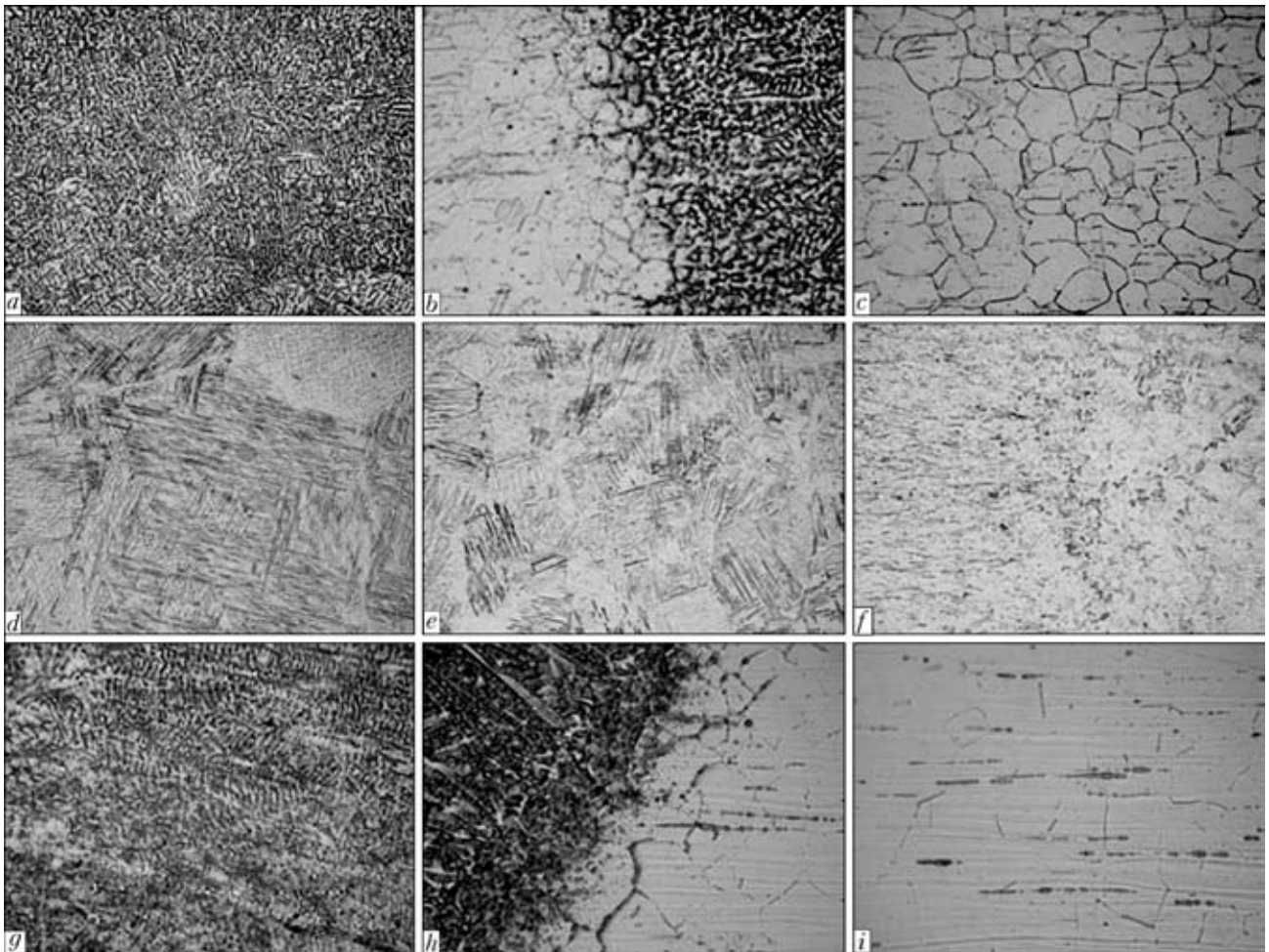


**Figure 4.** Microstructure ( $\times 320$ ) of butt joints of tubes from steel 304SS (*a-c*), PT-3V alloy (*d-f*) and monel alloy (*g-i*) made by EBW: *a, d, g* – central sections of weld metal; *b, e, h* – sections of fusion zone and coarse grain of the HAZ; *c, f, i* – regions of HAZ and base metal boundary

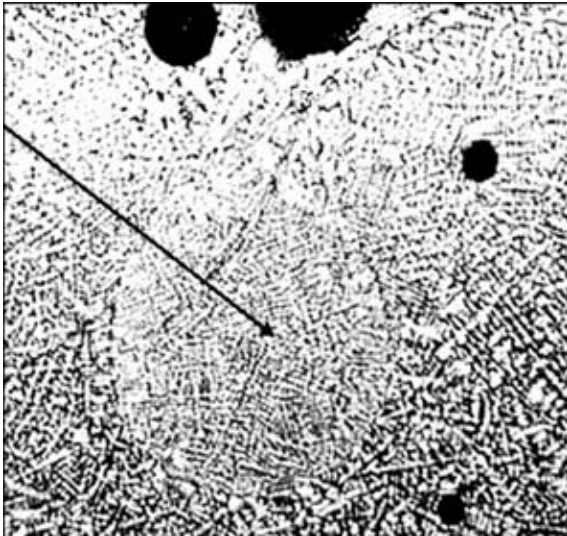


**Figure 5.** Microstructure ( $\times 320$ ) of weld metal of a joint from monel alloy with porosity and a void, filled with solidified liquid metal after welding (along the arrow)

welding with this process the HAZ is more ductile compared to the tube base metal to which no thermal impact was applied.

Investigations of polished sections of joints from steel 304SS, titanium alloy PT-3V and monel alloy showed that such nonmetallic inclusions as oxides, sulphides, silicates, etc. were found in the base metal of steel 304SS and monel alloy, whereas practically no nonmetallic inclusions were present in titanium alloy PT-3V.

Microstructure of base metal and weld metal from 304SS steel (Figure 4, *a-c*) is mostly austenitic with a small quantity of  $\delta$ -ferrite. Base metal of titanium alloy PT-3V (Figure 4, *f*) consists of grains of  $\alpha$ -phase, elongated along the rolling stock texture, and that of weld metal and HAZ consists of grains of  $\alpha'$ -phase (Figure 4, *d, e*). Microstructures of joints from PT-3V alloy have no clearcut fusion line (Figure 4, *e*). This promotes an improvement of ductility of HAZ section and inhibits crack propagation from the base metal into the HAZ and the weld (Figure 3, *b*). A clearcut boundary between the HAZ and base metal is also observed (Figure 4, *f*). Microstructure of base metal and weld metal of monel joints is similar to that of pure nickel [14] and has a single-phase composition of nickel-based solid solution (Figure 4, *g, i*). Small

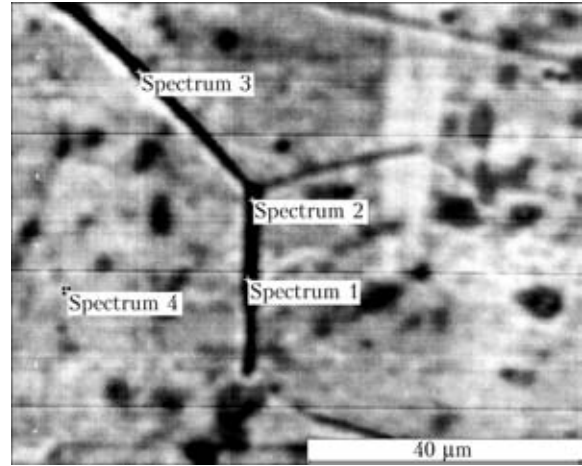


**Figure 6.** Interlayers along the grain boundaries in coarse grain zone (at the fusion line)

additives of iron and silicon, as well as copper but in larger quantities, are present in the solution and form no separate phases.

When studying the macro- and microstructures of welded joints of monel alloy produced by orbital EBW in a single pass, the weld metal demonstrated coarse and fine porosity (Figure 5). In addition, oval voids filled with metal with solidified submicrostructure are also observed (along the arrow). No such defects were found in welds made in two passes.

Formation of pores and cavities in joints from monel alloy is attributable to proneness of nickel and its alloys to formation of porosity in welding [15], as well as to a feature of hydrodynamic processes of liquid metal transfer in a narrow weld pool.

On the other hand, investigation of microstructure of HAZ metal from the fusion line to the boundary with the base metal in monel alloy joints also allowed revealing the presence of dark interlayers along the grain boundaries both in the HAS metal and in the base metal, which is not observed in the weld metal (see Figure 4, *g-i*).

Composition of these interlayers was studied in a scanning electron microscope JSM-35CF (JEOL, Japan), fitted with energy-dispersion microanalyzer system INCA 350. Analysis of electronographs confirmed the presence of dark interlayers along the grain boundaries (Figure 6), the composition of which was determined using INCA 350 microanalyzer.

**Table 4.** Distribution of microhardness of tube welded joints produced by orbital EBW, MPa

#	Material	Number of passes	Base metal	HAZ			Weld	
				Recrystallized zone	Double recrystallized zone	Overheated zone	Fusion zone	Weld middle
1	304SS	1	3060	2920	2500	2130	2380	2430
2		2	2980	2530	2300	2050	2300	2430
3	PT-3V	1	2740	2480	2350	2300	2300	2740
4		2	2700	2390	2300	2200	2300	2700
5	Monel	1	1700	1650	1600	1550	1600	1740
6		2	1620	1600	1580	1550	1540	1580



Obtained results of examination of these areas are indicative of an increased content of oxygen (up to 2.0 %), as well as aluminium (up to 0.4 %) and titanium (up to 0.2 %) compared to their content in the grain body. Apparently, predominant oxidation with formation of  $Al_2O_3$  and  $TiO_2$  oxides runs along the grain boundaries. Presence of oxides along the grain boundaries can promote an increase of stress intensity in these regions, that under certain conditions may lead to fracture propagation through them, which is a possible reason for the obtained results of rupture testing of tubular joints from monel alloy (Table 3).

Results of metallographic investigations are in good agreement with the results of rupture tests. Welds made in two passes have less nonmetallic inclusions and pores compared to single-pass welds and higher strength values, respectively.

Microhardness of the produced joints in the regions of weld metal, HAZ and in the base metal has different values, depending on the material and pass number (Table 4). For the studied materials microhardness after the second pass is more stable, but in the coarse grain section near the fusion line it is somewhat lower than after the first pass.

Investigations of chemical inhomogeneity by X-ray microprobe analysis showed that the uniform and equal distribution of alloying elements in welded joints from steel 304SS, titanium alloy PT-3V and monel alloy is independent on the number of passes.

Thus, orbital EBW process allows producing sound welded joints of tubes from stainless steels, monel alloy and titanium alloys.

1. Masubishi, K. (1989) Space technologies of joints developed in the USA. *Tekhnika Sborniki i Soedineniya*, **8**, 103–108.
2. Suezawa, E. (1989) Space stations and colonies. *Ibid.*, **9**, 66–75.
3. Paton, B.E., Dudko, D.A., Lapchinsky, V.F. et al. (1973) Application of welding in repair of space objects. *Kosmich. Issled. na Ukraine*, Issue 9, 3–9.
4. Paton, B.E., Lapchinsky, V.F. (1998) *Welding and related technologies in space*. Kiev: Naukova Dumka.
5. Paton, B.E., Lapchinsky, V.F., Stesin, V.V. et al. (1977) Some principles of construction of equipment for technological operations in space. In: *Subject Coll. of 6th Gagarin Readings on Technology in Space*. Moscow.
6. Ternovoj, E.G., Bulatsev, A.R., Solomijchuk, T.G. et al. (2010) Repair of pipelines using orbital TIG welding inside inhabited space objects. *The Paton Welding J.*, **4**, 10–13.
7. Paton, B.E. (2000) Space technologies on the threshold of the third millennium. *Ibid.*, **4**, 2–4.
8. (2000) *Space: technologies, materials, structures*. Ed. by B.E. Paton. Kiev: PWI.
9. Abramov, E.V., Lyashenko, V.I., Semenov, V.A. (1975) *Automatic welding of steel and titanium thin-wall tubes: Advanced methods of treatment of metals and alloys*. Leninograd: LDNTP.
10. (1978) *Welding in machine-building: Refer. Book*. Vol. 1. Ed. by N.A. Olshansky. Moscow: Mashinostroenie.
11. Grinenko, V.I., Belkin, S.A., Astafurova, N.I. (1963) Position butt welding of pipes of steel 1Kh18N9T by self-compression method. *Svarochm. Proizvodstvo*, **10**, 27–29.
12. Roshchin, V.V., Akulov, L.I., Grinenko, V.I. et al. *Self-compression method of welding*. USSR author's cert. 212409. Int. Cl. B 23K 9/16, 37/2. Publ. 05.05.1968.
13. Roshchin, V.V., Uschenko, Yu.S., Bukarov, V.A. et al. (1985) Properties of weld joints made by self-compression method. *IW Doc. XII-901-85*.
14. Maltsev, M.F., Barsukova, T.A., Borin, F.A. (1960) *Metallography of nonferrous metals and alloys*. Moscow: Metallurgizdat.
15. Bagryansky, K.V., Kuzmin, G.S. (1963) *Welding of nickel and its alloys*. Moscow: Mashgiz.

## ELECTRON BEAM WELDING OF HEAT EXCHANGERS WITH SINGLE OR DOUBLE REFRACTION OF THE ELECTRON BEAM

L.A. KRAVCHUK, V.I. ZAGORNIKOV and I.A. KULESHOV  
E.O. Paton Electric Welding Institute, NASU, Kiev, Ukraine

Selection of energy and time parameters of the electron beam in EBW of tubes to tubesheets of heat exchangers from titanium and the possibility of making a circumferential weld by applying single and double refraction are considered, as well as rotation of the electron beam around the butt using a deflection system. The paper gives the schematic of welding in common vacuum and modes ensuring formation of fillet weld without reducing the pass section of an up to 40 mm diameter tube, including the case when the tubes extend above the tubesheet level.

**Keywords:** EBW, electron beam, heat exchanger, tube and tubesheet, welding schematic, single and double refraction, deflecting system, circular and local scan

At present two fundamentally different technologies of EBW of tubes to tubesheet have become accepted in industry. The difference between them consists in space-time orientation of the electron beam relative to tubesheet plane [1, 2]. In case of single refraction of the electron beam and its rotation around the butt joint by the deflection system relative to a stationary

item (Figure 1, a) there is a dependence between penetration depth  $h_{pen}$ , distance from beam focusing plane to item  $f_b$ , tube diameter  $D_p$ , and refracted beam deviation in the weld root from tube-to-tubesheet butt  $\Delta k$ :

$$\Delta k = \frac{D_p}{2f_b} h_{pen}$$

It is seen from this dependence that deviation of refracted electron beam in the weld root from tube-to-tubesheet butt increases with the increase of values